Research and Foundation of Inversion Lattice Potential of Pd

REN Xianli, CHEN Song*, XIE Ming, LI Muyang, WANG Song, HU Jieqiong, WANG Saibei
(Sate Key Laboratory of Advanced Technologies for Comprehensive Utilization of Platinum Metal, Kunming Institute of Precious Metals, Kunming 650106, China)

Abstract: The lattice cohesive energy curve of palladium was obtained through first-principles calculations based on local-density approximation theory(LDA). The accurate inversion potential curve was generated through Chen-Möbius inversion method. Based on the fitting results of different potential function, the double-exponential function to fit the inversion potential curve was presented. The phonon spectra of palladium were calculated through using the inversion potential data, the embedded atom method(EAM) potential theory and first principle method respectively to verify the reliability of the inversion potential. The tendency of these curves is consistent, which indicates that the inversion potential can reflect the interaction between atoms efficiently. Meanwhile, inversion potential method needs less time in the computation comparing with the EAM potential method, pointing out the inversion method has great advantage in the amount of calculation. In addition, thermal expansion coefficient, including elastic modulus and Grüneisen constant were calculated based on the fitting function and parameters. The results are in good agreement with experiment results, which implies that the inversion potential is accurate.
Key words: palladium; first-principles; accurate inversion potential; lattice inversion
CLC number: TG146.3^{+}4 **Document code:** A **Article ID:** 1004-0676(2017)S1-0028-07

钯的反演势的构建与研究

任县利，陈 松*，谢 明，李慕阳，王 松，胡洁琼，王塞北
(昆明贵金属研究所 稀贵金属综合利用新技术国家重点实验室，昆明 650106)

摘 要：以面心立方金属钯为研究对象，基于第一性原理中的局域密度近似理论(LDA)，计算了不同晶格长度下的原子间内聚能并得到其原子内聚能曲线。通过陈-莫比乌斯晶格反演势理论，得到了精确的反演对势曲线。采用不同势函数对该曲线拟合，通过对拟合效果的对比和分析，提出了全局精度较高的双指数型势函数。同时，分别采用第一性原理方法，原子嵌入势(EAM)方法和反演势数据计算了钯的声子谱。比较声子谱曲线发现，曲线的变化趋势是相似的，说明反演势可以合理的反应原子间相互作用。并且反演势方法所需的计算时间明显少于 EAM 势方法，说明反演势方法在计算量上有明显优势。最后，计算了金属钯的热膨胀系数，弹性模量和格林乃森常数等物理量。计算结果与实验数据基本符合，表明构建的钯的反演势是准确有效的。
关键词：钯；第一性原理；精确反演势；晶格反演

The potential function, as foundation of molecular dynamics method, directly determines the accuracy and reliability of the simulation calculation consequence. Empirical many-body potential models

收稿日期：2017-08-30
基金项目：国家自然科学基金(51267007, 51461023, U1602275, U1602271)、云南省技术创新人才项目(2016HB024)、云南省自然科学基金(2010CD126, 2012FB195, 2015FA042)。
第一作者：任县利，男，硕士，研究方向：计算材料学。E-mail：renxianli_1@163.com
*通讯作者：陈 松，男，博士，研究员，研究方向：计算材料学。E-mail：cs@ipm.com.cn

include adjustable parameters which should be determined by fitting to the experimental data of the involved systems, for example, the EAM potential. Considering the experimental data should be obtained in different physical conditions and for different types of materials the potential models are various, the general applicability of empirical many-body potential is not good. Chen's lattice inversion theory is based on the Möbius transformation in number theory, through strict mathema-tical proof without any experiential factors. Generated inversion potential is strict and accurate. Chen's lattice inversion method has been in common use to achieve the pair potentials based on the first-principles calculations, including the fields about rare earth transition intermetallic compounds, metal-ceramic interfaces, ionic crystals and semiconductors [1-4]. As face centered cubic (FCC) metal, Palladium has metallic bonds, and electron distribution between atoms is spherically symmetric. Inversion potential function is expressed as spherically symmetric form. Meanwhile, the accuracy of inversion potential is affected by the amount of inversion coefficient and fitting functions [5-6]. However, in related studies, the inversion coefficient amount is less, the overall performance of fitting function still needs to be improved. Using the first principles method and Chen's lattice inversion theory, the accurate curve of inversion potential of Palladium is constructed [7]. The overall precise analytical expression of the double-exponential function equation is presented [8-9]. Then these calculated results are analyzed and applied.

1 Computational details

1.1 The construction of inversion lattice potential

The calculations are performed through plane wave pseudo-potential method based on density function theory in the Cambridge Sequential Total Energy Package (CASTEP) package. The electron exchange and correlation are treated within the local-density approximation (LDA) using the Perdew and Zunger (CA-PZ) function. The Brillouin-zone is sampled by a $12\times12\times12$ k-point mesh. The cutoff energy is set to 310 eV to obtain accurate total energy. The SCF tolerance is set as 1×10^{-6} eV/atom. The valence electron configuration of Pd is $4d^{10}$. The spin polarization is not considered [10-11]. Isolated atomic ground state energy is obtained through calculating energy in the unit cell. The calculated ground state energy curve is shown in Fig. 1. The curve is fitted by the following function:

$$\varphi(r)=E_0+D\exp[-(r-R_0)/\varepsilon] \quad (1)$$

where E_0 is the ground state energy of isolated atom and E_0^{Pd}=-795.36335 eV.

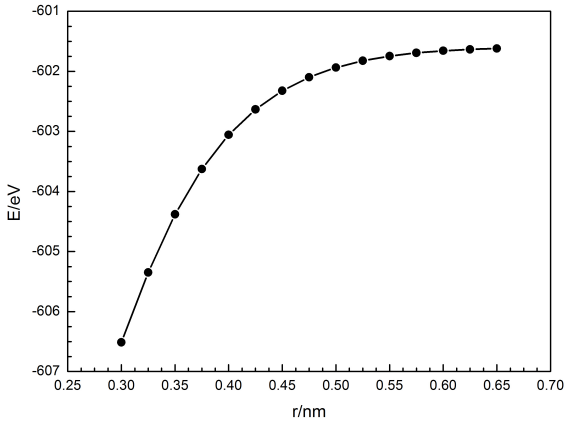

Fig.1 Relationship between the isolated atomic energy and the nearest atom distance curve of Pd

图 1　Pd 的单原子能和最近原子距离之间的关系

The lattice cohesive energy in different atomic distances are calculated with distance ranging from 0.21 nm to 0.81 nm. The curve, as shown in Fig.2, is achieved after the value of single atom cohesive energy subtracting the isolated atom ground state energy.

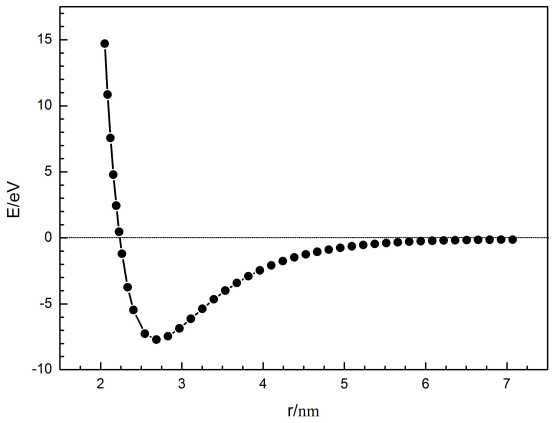

Fig.2 The lattice cohesive energy curve of Pd

图 2　Pd 的晶格内聚能曲线

Based on the Chen's inversion theory, one thousand inversion coefficients in FCC lattice structure has been calculated with first 60 coefficients exactly matching the numerical table given by Chen [12]. And the pair potential between different atoms is written as:

$$\varphi(x)=2\sum_{n=1}^{\infty}I(n)E(b(n)x) \tag{2}$$

where $I(n)$ is inversion coefficient depending on the structure, and can be written as

$$\sum_{b(n)|b(m)}I(n)r\left(b^{-1}\left[\frac{b(m)}{b(n)}\right]\right)=\delta_{m1} \tag{3}$$

The curve of lattice inversion potential is shown in Fig.3.

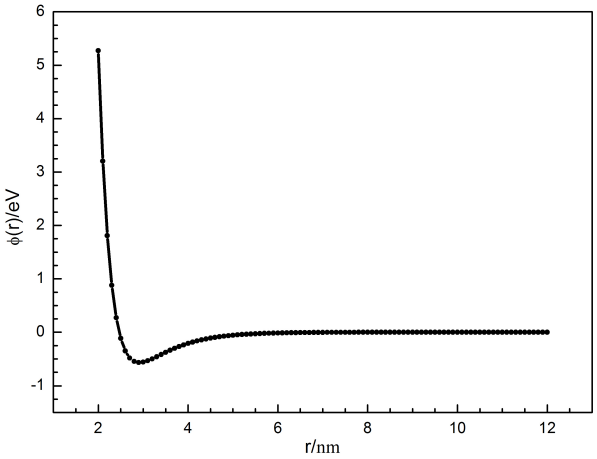

Fig.3 The lattice inversion potential curve of Pd

图 3 Pd 的晶格反演势

1.2 The fitting of inversion potential function

Fitting quality can be estimated by the coincidence quality between calculated points chain with fitting curve. Different potential functions, such as Rose function, L-J function, Morse function and the new double-exponential potential function proposed in the work are used to fit the lattice inversion potential curve shown in Fig. 3. Parameter b that represents correlation coefficient changing from 0 to 1 is obtained through using above functions. If the value of b is close to 1, meant that the fitting performance is excellent and the fitting function is accurate.

1.2.1 The fitting of Rose function

The form of Rose function is:

$$\varphi(r)=-D[1+\alpha(r-R_0)]\exp[-\alpha(r-R_0)] \tag{4}$$

where D, R_0, and α represent parameters generated from fitting processing, $\varphi(r)$ represents the inversion potential energy, α represents the distance between atoms. The obtained b is 0.999. The fitting curve matches the points chain very well in the short distance [13]. However, when the distance ranges from 0.2nm to 1.2nm, the overall performance is not well.

1.2.2 The fitting of L-J function

The equation is expressed as:

$$\varphi(r)=4\varepsilon[(\frac{n}{m-n})(\frac{\sigma}{r})^m-(\frac{m}{m-n})(\frac{\sigma}{r})^n] \tag{5}$$

The value of correlation coefficient b is 0.99779. Under close magnification the function curve matches the points well in the long range and short range except the curve segment nearby the knee point, meant the overall perfor-mance is not well.

1.2.3 The fitting of Morse function

The equation is expressed as:

$$\varphi(r)=D[\exp(-2\alpha(r-R_0))-2\exp(-\alpha(r-R_0))] \tag{6}$$

The parameters are listed in Tab.1.

Tab.1 Fitting parameters of Morse potential function

表 1 拟合得到的摩尔斯势参数

Element	D/eV	α/(1/nm)	R_0/nm
Pd	0.58728	0.157174	0.290559

The value of correlation coefficient b is 0.99978. The fitting function performs well in the short range and long range except the curve segment nearby the knee point when zoomed in the curve, which meant the overall performance still need to be improved. Whereas the Morse potential function has been widely used in the pair potential research, comparing the calculation results with the existing data [14] is meaningful. The parameters of Morse function is given in Tab.2.

Tab.2 Parameters of Morse potential function

表 2 摩尔斯势参数

Element	D/eV	α/(1/nm)	R_0/nm
Pd	0.4761	0.16189	0.2890

The value of R_0 and α are basically accorded, while the value of D has larger difference. The main reason is the temperature chosen by Table 1 is 0 K, while Table 2 is calculated under gas state. The value of R_0 is determined by the nearest atom distance at equilibrium state. Although lattice constant will change with the action of atomic vibrations as temperature rose, the equilibrium position remains unchanged. The value of α is determined by the second derivative of potential function with respect to r. Both of them are unrelated to the temperature chosen by the potential function. The value of D is relevant to the temperature which relates the difference of minimum value of inversion potential [15]. So the calculated results are fundamentally accurate.

1.2.4 The fitting of double-exponential potential function equation

The double-exponential potential function is proposed in this work to improve the accuracy in the fitting [16]. The equation containing five parameters is:

$$\varphi(r) = D_1 \exp[-\alpha(r - R_0)] - D_2 \exp[-\beta(r - R_0)] \quad (7)$$

These parameters are listed in Tab.3.

Tab.3 Parameters of double-exponential function

表 3 双指数函数的参数值

Element	D_1/eV	α/(1/nm)	D_2/eV	β/(1/nm)	R_0/nm
Pd	0.9949	0.346549	1.37009	0.132804	0.261458

The value of b is 1, indicating that the fitting quality is excellent. When zoomed in the curve, the overall coincidence in the distance ranging from 0.2 nm to 1.2nm is perfect. It is certain to provide strong precision support for the following calculation.

2 Application and Analysis

2.1 The analysis of the phonon spectra of Pd

To verify the reliability of the inversion potential, the phonon spectra of Palladium is calculated through using inversion potential data, EAM potential theory and first-principle method respectively, as shown in Fig.4.

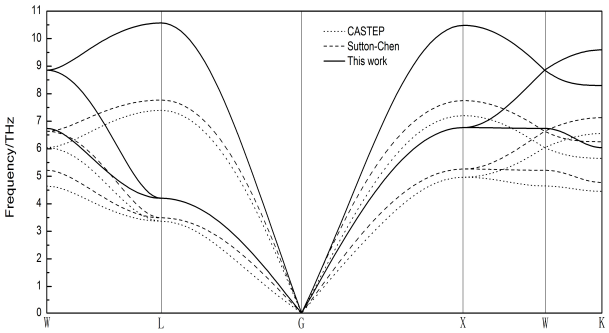

Fig.4 The phonon spectra of Pd

图 4　Pd 的声子谱

The coordinate of these main symmetric points in the Brillouin Zone are G (0, 0, 0), X (0.5, 0, 0.5), W (0.5, 0.25, 0.75), K (0.75, 0.375, 0.375), L (0.5, 0.5, 0.5). The tendency of these curves is consistent, meant inversion potential can reflect the interaction between atoms efficiently, though there are some deviation in the value of frequency, especially in the high frequency. The EAM potential method needs 77 times more time in the computation comparing with inversion potential method, indicating that the inversion method has great advantage in the amount of calculation. As for EAM potential function, it has a wide choice of function forms and more empirical factors. Its equation is deduced based on the Rose potential function, which leads to the unreliable calculation results when the atom distance is away from the equilibrium position, especially in the high temperature circumstance or in the process of volatile. Yet inversion potential based on the number theory, through strict mathematical proof, is an overall accuracy potential. It is effective and reliable.

2.2 The verification and calculation of the potential function

Eq.(8) is used to fit the lattice cohesive energy curve as shown in Fig.2. Fitting parameters are shown in Tab.4. The value of correlation coefficient b is 0.99996.

$$u(r) = D_1 \exp[-\alpha(r - R_0)] - D_2 \exp[-\beta(r - R_0)] \quad (8)$$

Tab.4 Fitting parameters of lattice cohesive energy curve

表 4 拟合得到的晶格内聚能曲线参数

Element	D_1/eV	α/(1/nm)	D_2/eV	β/(1/nm)	R_0/nm
Pd	-6.06882	0.138073	-1.33602	0.367134	0.294621

The first derivative equals to zero of the lattice cohesive energy with respect to the relative distance r, which leads to the nearest atom distance in equilibrium state of 0 K. The value of the nearest atom distance of Pd is r_0^{Pd}=0.2712419 nm. Physical quantities such as linear expansion coefficient, bulk modulus, Young's modulus, and Grüneisen constant are calculated. Then the calculation results are compared with experimental data.

2.2.1 The calculation of linear expansion coefficient

The calculation method is mainly based on the Boltzmann statistics equation, which can calculate the atomic average thermal vibration displacements at different temperature, and can be written as

$$\bar{\delta} = \frac{\int_{-\infty}^{\infty} \delta e^{-V/k_B T} d\delta}{\int_{-\infty}^{\infty} e^{-V/k_B T} d\delta} \tag{9}$$

Where δ=r-r_0, r_0 represents the nearest atom distance at 0 K. Considering each atom has a certain size, r_0 must be a value varies from α to ∞, where α represents the ionic radius, and α_{Pd}=0.073 nm, resulting in:

$$\bar{\delta} = \frac{\int_{a}^{\infty} r e^{-V(r)/k_B T} dr}{\int_{a}^{\infty} e^{-V(r)/k_B T} dr} - r_0 \tag{10}$$

The linear expansion coefficient is a one-dimensional quantity, and $V(r)$ is the One-dimensional quantity of lattice cohesive energy, while $u(r)$ is the three-dimensional quantity of lattice cohesive energy. So the relationship between $V(r)$ and $u(r)$ is $V(r)$=$u(r)$/3. The average thermal vibration displacements under the temperature range from 273 to 373 K are calculated using self-compiled programs. The curve is shown in Fig.5.

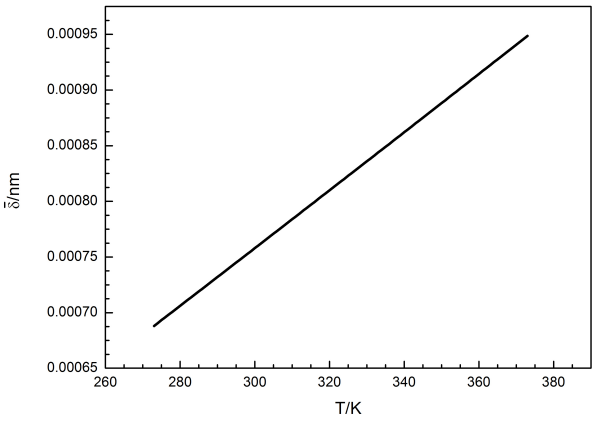

Fig.5 Relationship between atomic average thermal vibration displacements and temperature curve of Pd

图 5 Pd 的平均热震动位移与温度的关系

Based on the equation:

$$\alpha_L = \frac{1}{r_0}\frac{d\bar{\delta}}{dT} \tag{11}$$

The linear expansion coefficient (273~373 K) is calculated as α_L^{Pd}=0.960257×10^{-5} K^{-1}. Comparing with the experimental data α_{Pd}=1.1×10^{-5} K^{-1} [17], the relative error is 12.7%. The main reason is the contribution of metal free electron gas has not been considered. According to Grüneisen equation:

$$\gamma = \frac{\kappa \alpha_V V}{C_V} \tag{12}$$

Where κ represents bulk modulus, α_V represents volumetric expansion coefficient, γ represents Grüneisen constant, C_V represents the specific heat at constant volume, and the relationship between α_V and α_L is α_V=3α_L, the total specific heat of metal is the sum of lattice specific heat and electron specific heat, and can be written as:

$$C_V^{total} = C_V^{lattice} + C_V^{electron} \tag{13}$$

When the temperature is higher than the Debye temperature, $C_V^{lattice}$ plays the leading roles in the total specific heat, while at lower temperature, $C_V^{electron}$ will make significant contri-bution to the value of total specific heat. At the temperature ranging from 273 K

to 373 K, the influence of metal free electron gas cannot be ignored, or the calculation results will be lower than the experimental data.

However, the calculation method above-mentioned is meaningful. In the other report, the linear expansion coefficient was calculated through calculating the phonon spectra based on linear response theory and first principle method [18]. The computation is complicated. The method combining Boltzmann statistics equation with accuracy fitting of lattice cohesive energy curve is more practical and effective. There are less computation amount, less steps in the process, and the results are accurate.

2.2.2 The calculation of bulk modulus

The relationship between bulk modulus and lattice cohesive energy [19] is:

$$\kappa = V(\frac{\partial^2 U}{\partial V^2}) \tag{14}$$

Where U is the total energy of 1 mol atoms. V is the volume occupied by 1 mol atoms in the FCC structure, resulting in:

$$\kappa = \frac{\sqrt{2}}{9r}\frac{\partial^2 u}{\partial r^2} - \frac{2\sqrt{2}}{9r^2}\frac{\partial u}{\partial r} \tag{15}$$

And $u(r)$ can be calculated based on Eq.(8):

$$\kappa = \frac{\sqrt{2}}{9r}\left\{\alpha^2 D_1 \exp[-\alpha(r-R_0)] - \beta^2 D_2 \exp[-\beta(r-R_0)]\right\}$$
$$-\frac{\sqrt{2}}{9r^2}\left\{\alpha D_1 \exp[-\alpha(r-R_0)] - \beta D_2 \exp[-\beta(r-R_0)]\right\} \tag{16}$$

Considering the calculation of bulk modulus at room temperature is more practical. The average thermal vibration displacement at 293 K is $\bar{\delta}_{Pd}$=7.4×10^{-4} nm using Eq.(10). Meanwhile $r_0'= r_0+\bar{\delta}$, where r_0' represents the nearest atom distance at equilibrium state of 293 K, we get $r_0'^{Pd}$=0.2719819 nm. Then the value of bulk modulus at room temperature is κ_{Pd}=2.376046×10^{11} N·m^{-2}. Whereas the experimental data is κ_{Pd}=1.87×10^{11} N·m^{-2} [17], the relative error is 27%, meant the calculation method is effective and practical.

2.2.3 The calculation of Young's modulus

According to the relationship between Young's modulus and cohesive energy function:

$$Y = \frac{1}{6}\frac{\mathrm{d}U/\mathrm{d}V}{\mathrm{d}r/r} \tag{17}$$

Whereas the Young's modulus is a One-dimensional physical quantity, cohesive energy $U(r)$ is a scalar quantity and the stress of per unit area $\mathrm{d}U(r)/\mathrm{d}V$ is a vector quantity, Eq.(17) should multiply 1/6 in the right-hand side, then:

$$Y = \frac{\sqrt{2}}{18r}\frac{\partial^2 u}{\partial r^2} - \frac{2\sqrt{2}}{18r^2}\frac{\partial u}{\partial r} \tag{18}$$

The average value of Young's modulus at 293 K is calculated as Y_{Pd}=1.188023×10^{11} N·m^{-2}. Comparing with Y_{Pd}=1.21×10^{11} N·m^{-2} [17], the relative error of Pd is 1.8%.

2.2.4 The calculation of Grüneisen constant

Based on Eq.(12), the value of κ and α_V calculated above, and equation:

$$V = \frac{N_A}{4}\left(\sqrt{2}r_0\right)^3 \tag{19}$$

Where N_A represents the Avogadro's number, the value of Grüneisen constant γ at 293 K is achieved as γ_{Pd}=2.26. Comparing with γ_{Pd}=2.2 [17], the relative error is 2.7%. The result is accurate and effective.

3 Conclusions

Inversion potential of palladium is studied using the first-principles and Chen's theory[20]. The double-exponential function has been turned out to be an accurate and effective function to fit the inversion potential curve. Its excellent performance in the overall accordance will provide strong precision support for the following calculation. Then the phonon spectra are calculated through using three methods. Results show that the inversion potential is efficiently and has great advantage in the amount of computation [21]. Meanwhile, the method combining Boltzmann statistics equation with accuracy fitting of lattice cohesive energy curve is proposed to calculate the thermal expansion coefficient. The bulk modulus, including Young's modulus and Grüneisen constant in different temperature can be calculated according to the value of atomic average thermal vibration displacements. The relative error of these three quantities at room temperature is 27%, 1.8% and 2.7% respectively, indicates the calculation method and results are effective and reliable.

References:

[1] LONG Y, CHEN N X . Theoretical study of (Ag, Au and Cu)/Al_2O_3 interfaces[J]. Journal of physics-condensed matter, 2009, 21(31): 315003.

[2] SONG H Q, SHEN J, QIAN P, et al. Interfacial for Ag/GaN(0001) interfaces by inversion of adhesive energy [J]. Physica B, 2013, 431: 97-101.

[3] ZHANG C H, HUANG S, LI R Z, et al. Effects on mechanical properties of refractory metal doped Ti_3Al alloy[J]. International journal of modern physics B, 2013, 27(26): 1350147.

[4] ZHANG C H, HUANG S, SHEN J, et al. Chen's lattice inversion embedded-atom method for Ni-Al alloy [J]. Chin phys B, 2012, 21: 113401.

[5] 夏璐, 陈松, 陆建生, 等. 分子动力学模拟用贵金属势函数的应用与发展[J]. 贵金属, 2013, 34(4): 82-90.

[6] 万纾民. 固体中原子间相互作用势能函数与碱金属、碱土金属弹性的电子理论[J]. 中国科学(A 辑), 1987, (2): 170-178.

[7] 夏璐, 陈松, 陆建生, 等. 分子动力学模拟用贵金属势函数的应用与发展[J]. 贵金属, 2014, 35(1): 31-35.

[8] Wang Y D, Chen N X. Atomistic study of misfit dislocation in metal/SiC(111) interfaces[J]. Phys. condens matter, 2010, 22: 135009-135018.

[9] XIA L. The foundation and application of inversion potentials for the PtRh alloys[D]. Kunming: Kunming University of Science and Technology, 2013.

[10] LIU S J, SHI S.Q, HUANG. H. Interatomic potentials and atomistic calculations of some metal hydride systems[J]. Journal of alloys and compounds, 2002, 330: 64-69.

[11] 张建民, 吴喜军, 黄育红, 等. fcc 金属层错能的 EAM 法计算[J]. 物理学报, 2006, 55(1): 393-397.

[12] CHEN N X. Möbius inversion in physics[M]. Singapore: World Scientific Publishing Co Pte Ltd, 2012.

[13] 谢谦, 黄美纯. 完整晶格的晶向族描述与晶格和[J]. 厦门大学学报(自然科学版), 1994, 33(1): 36-42.

[14] FLAHIVE P G, GRAHAM W R. Pair potential calculations of single atom self-diffusion activation energies[J]. Surface science, 1980, 91:449-462.

[15] ZHANG C H, HUANG S, LI R Z, et al. Structural and mechanical properties of Fe-Al compounds: An atomistic study by EAM simulation [J]. Intermetallics, 2014, 52: 86-91.

[16] 陈松, 胡昌义, 郭俊梅, 等. Ir/Mo 互扩散研究[J]. 稀有金属材料与工程, 2005(6): 916-919.

[17] BRANDES E A, BROOK G B, Smithells metals reference book: 7ed[M]. Oxford: Reed Educational Zand Publishing Ltd, 1992.

[18] 胡洁琼, 潘勇, 谢明. RhZr 相结构稳定性和电子结构性质的第一性原理研究(英文)[J]. 中国有色金属学报(英文版), 2011, 21(10): 2301-2305.

[19] LIU C, ZHOU T. The expansion coefficient and elastic modulus of crystal with fcc structure[J]. Journal of Southwest China Normal University, 2006, 31(5): 83-87.

[20] 刘泽光, 陈登权, 罗锡明, 等. 微电子封装用金锡合金钎料[J]. 贵金属, 2005, 26(1): 62-65.

[21] 陈松, 耿永红, 王传军,等. 磁控溅射用 CoCrPt 系靶材制备技术研究进展[J]. 贵金属, 2013, 34(1): 74-78.